ORIGINAL PAPER

Consideration of geomorphic indices in assessment of relative active tectonics in a part of seismogenic compressional Kashmir Basin

Umair Ali[1] · Syed Ahmad Ali[1] · Maqbool Yousuf[2] · Qazi Akhter Rasool[3] · Mukeem Ahmad[1] · Ishtiyaq Ahmad[2]

Abstract
The area is located in seismically active belt NW Himalaya resultant of collision between Indo-Eurasian plates. Due to presence of faults, folds, and active tectonics of Himalayan region, mountain front designs, behavior of fluvial system, and landform development have been extensively shaped and sculptured by tectonic activity. In the present study, the assessment of relative tectonic activity is carried out in the Sukhnag catchment using geomorphic indices: the stream length-gradient index (SL), basin asymmetry (Af), hypsometric integral (Hi), valley floor width-valley height ratio (Vf), basin shape (Bs), and mountain-front sinuosity (Smf). These indices were used to compute relative tectonic activity (Iat) among 14 sub-watersheds; class 1 (very high relative tectonic activity, nill); class 2 (high, SF 1, 2, 5, 6, 9, and 11); class 3 (moderate, SF 3, 4, 7, 8, and 13); and class 4 (low, SF10, 12, and 14). Tectonic activity is high in sub-watersheds where various tectonic imprints like stream deflections, straightness of streams, deep valleys, steep slopes, and lineaments of tectonic significance showed their presence; these lineaments showed linear trend with the dominant zones of earthquake epicenters in the surroundings. Thus, the areas with higher tectonic activity are analyzed by geomorphic indices, supported by presence of various geomorphic expressions, tectonic imprints and field evidences.

Keywords Geomorphic indices · Relative tectonic activity · Sukhnag catchment · Kashmir Basin · Himalaya

Introduction

The Himalayan arc is developed by the collision of the Indian and Eurasian plate onset at ~ 55 Ma (Gansser 1964; Molnar and Tapponnier 1975; Nakata 1972, 1986; Valdiya 1980; Nakata et al. 1984; Srikantia and Bhargava 1998; Thakur 1993, 2004; Jain et al. 2002, 2005), and consequent formation of Himalayan orogeny though subdued, has not yet ceased (Nakata 1989). Many active faults and neotectonic features have been reported (Bilham 2004, Valdiya 1992; Yousuf and Bukhari 2020a; Bali and Wani 2021) that have generated

major and great earthquakes (Ambraseys 2004; Philip and Virdi 2006). The geomorphological study of active tectonics in the late Pleistocene and Holocene are essential to earthquake hazard assessment in the tectonically active areas (Keller and Pinter 2002) like the Kashmir Basin which falls almost in highest earthquake zones (BIS 2002) with the presence of seismites (Ali and Ali 2018; Yousuf and Bukhari 2020a) and shows variable response to earthquake shaking compared to surrounding regions (Ali and Ali 2020; Yousuf et al. 2020; Yousuf and Bukhari 2020b). The vibration felt by the geophone in different directions is very different (e.g., Ma et al. 2018; Ma et al. 2019). Moreover, the several studies suggest a major NE-dipping thrust fault, Kashmir basin fault/Balapur fault in Kashmir basin (Ahmad et al. 2013; Ahmad and Bhat 2012; Shah 2013, 2015a b; Wani and Bali 2017; Wani et al. 2019). The Kashmir basin situated in the western part of Himalayan orogenic system is at ~ 100 km distance from the deformation front of the Himalaya (Nakata 1989; Kaneda et al. 2008; Meigs et al. 2010; Madden et al. 2010, 2011; Ahmad et al. 2013; Shah 2013; Ali and Ali 2017).

The geologic and geomorphologic processes that continuously work on the earth's surface resulted in different landforms (Crevenna et al. 2005; Bali et al. 2016). The quantitative

---

✉ Umair Ali
    umairgeo121@gmail.com

1   Department of Geology, Aligarh Muslim University,
     Aligarh 202002, India

2   Department of Civil Engineering, National Institute of Technology,
     Srinagar 190006, India

3   Department of Disaster Management, Pondicherry University,
     Pondicherry 605014, India

measurements of landforms are accomplished by calculation of geomorphic indices from topographic maps, digital elevation model, satellite imagery, aerial photographs, and field data (Toudeshki and Arian 2011; Wani et al. 2020). The drainage patterns and other anomalies evident on topographic maps, digital elevation models, and aerial photographs are helpful for structural interpretation (Howard 1967; Kurz et al. 2007; Gloaguen et al. 2007, 2008; Ali and Ali 2017), and were helpful in understanding the landscape evolution and recognize active tectonic movements (Riquelmea et al. 2003; Malik and Mohanty 2007; Bathrellos et al. 2009; Kamberis et al. 2012). Geomorphic indices of active tectonics such as stream gradient (Chen et al. 2003), hypsometric integral (Pike and Wilson 1971; Strahler 1952), and landform assemblage are applied to reveal relative active tectonics (Ohmori 1993). These indices are important indicators used for decoding landform responses to active deformation processes and as a reconnaissance tool to differentiate zones deformed by active tectonics (Keller and Pinter 2002; Chen et al. 2003). Therefore, in this study, geomorphic indices are calculated and supported by investigation of drainage anomalies and tectonic lineaments. Combination of geomorphic indices has given a single index (Iat) to identify the relative active tectonics in the 14 sub-watersheds of Sukhnag catchment Kashmir Basin, NW Himalaya.

Geological setup

In the vicinity of the Kashmir Basin, several known and famous thrusts such as Panjal thrust (MCT), Muree thrust (MBT), Riasi thrust (RT), and Balakot bagh fault (BBF) considered to be imbrications of the northward-rooted basal decollement known as the Main Himalayan Thrust (MHT) are present (Schelling and Arita 1991; Brown et al. 1996; DeCelles et al. 2001). In addition to these mountain-bounding thrust sheets, Balapur Fault (BF) (out-of-sequence fault) has been mapped in Pleistocene deposits of the Kashmir basin on Pir Panjal side (Ahmad and Bhat 2012). Past earthquake record and neotectonic movements along several faults in the region indicates that orogenic process are going on (Valdiya 1998, 2001). The study area extends from 33°54′ to 34°15′ N latitude and 74°15′ to 74°48′ E longitudes (Fig. 1). The headstreams of Sukhnag drain the Pir-Panjal range from the Nurpur Gali (4086 m) and the Chinamarg peak (4386 m) and also take care of the drainage of Toshamaidan. The Sukhnag Nala has a length of about 54 km. The Ferozpur Nala rises in the slopes of the Pir-Panjal range from the Jamianwali Gali (4084 m) and Apharwat (4143 m). The Sukhnag catchment has an area of ~975.98 km². Geologically, the study area shows quite diverse rock types ranging from Precambrian to Recent. The commonest of the rocks present in the area are Panjal traps, Limestones,

Karewas, and Alluvium. Panjal traps are lying in the extreme west, Karewas covers most areas in middle, and the recent Alluvium has covered areas surrounding the Jhelum River (Fig. 1). The south-western side of the Sukhnag is having high relief and steep slopes (> 35°). The north-eastern side has low relief and has a gentle slope (5° to 20°). The structural and geomorphological features control the direction of flow of tributaries present in the area. The main stream flows toward north-eastern direction originating from high mountains. The area shows great altitudinal variation approximately from 1500 to 4143 m which has well helped and contributed in development of drainage network.

Methodology

In the present study, the geomorphic indices were computed to highlight tectonically active areas and to infer the effect of tectonic activity in the landscape evolution (Ahmad et al. 2013; Bali et al. 2016). Geomorphic indices are used as basic investigation tool to recognize areas with rapid tectonic activity (Bull and McFadden 1977; Keller and Pinter 1996) supported by the investigation of tectonic lineaments, and drainage anomalies. Tectonic lineament analysis (Fig. 2) carried out with the application of different geospatial techniques supported by geomorphic manifestations associated with these lineaments at most of the places without the obliteration due to surface erosional processes (Ali and Ali 2017). Relation of tectonic features like faults and folds in the development of landscape were studied by analyzing surface profiles from digital elevation model and intensive field validation. Six geomorphic indices are applied to assess relative active tectonics (Iat) and to explain the tectonic deformation (Keller and Pinter 2002). These are stream length gradient index (SL) (Hack 1973), hypsometric integral (Strahler 1952), valley-floor width to height ratio (Vf) (Bull 1977; Bull and McFadden 1977; Bull 1978), mountain front sinuosity ratio (Smf) (Bull 1977; Bull 1978; Bull and McFadden 1977), basin asymmetry factor (AF) (Hare and Gardner 1985; Cox 1994), and basin shape index (Bs) (Ramírez-Herrera 1998; Cannon 1976).

Stream length gradient index (SL) was computed by formula: $SL = (\Delta H/\Delta L)/L$, where ΔH and ΔL are the difference in height and length between two points and L is the total length, measured from the divide to middle of that two points. The SL index was calculated in all 14 sub-watersheds along the main streams and was categorized into three classes: class 1 (SL≥500), class 2 (300≤SL<500), and class 3 (SL<300) (El Hamdouni et al. 2007). The hypsometric integral (Hi) was calculated by: $H_i = (H_{Mean} - H_{minimum}) / (H_{maximum} - H_{minimum})$, where the maximum and minimum elevation was directly taken and mean elevation was computed by averaging more than 50 elevation values uniformly distributed in the sub-watershed. The Hi values are not only useful to infer the
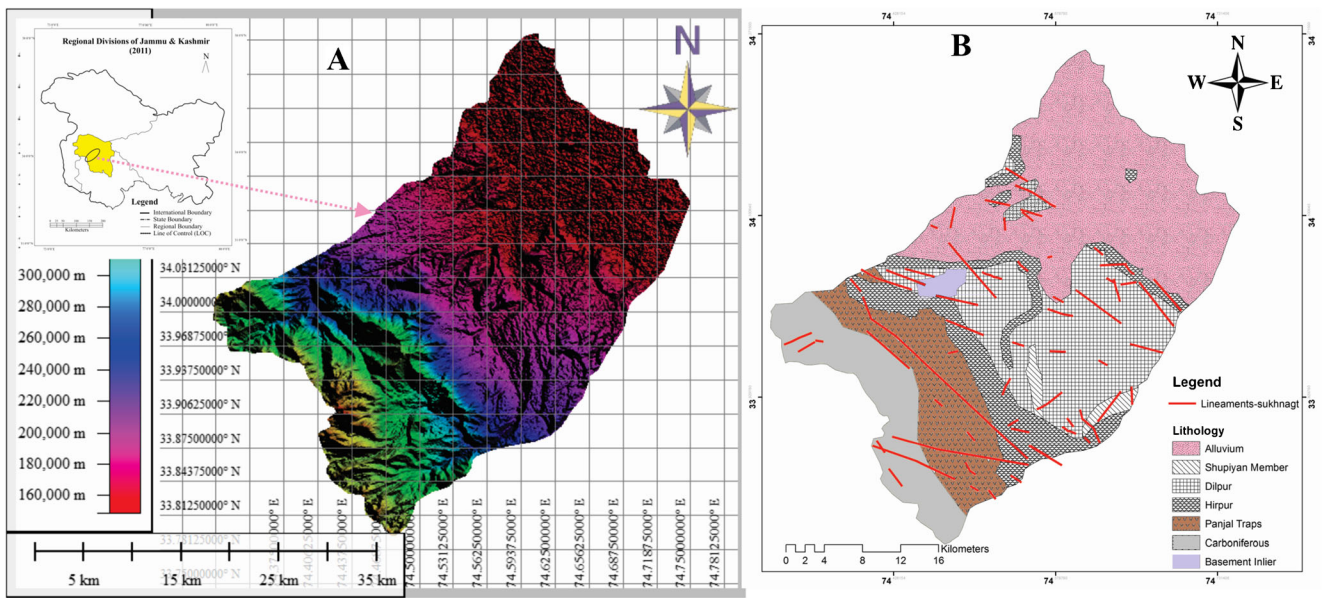
Fig. 1. Location map of study area situated in Kashmir basin (**a**), lithological variation in the area (**b**)

erosional stage, but highlights the lithological, climatic, and tectonic variation controlling the area (Huang and Niemann 2006; Molin et al. 2004). The H_i index was categorized into three classes based on convexity or concavity of the hypsometric curve: class 1 with convex curves ($H_i \geq 0.5$), class 2 with concave–convex curves ($0.4 \leq H_i < 0.5$), and class 3 with concave curves ($H_i < 0.4$). The valley floor width to height ratio was computed along the cross section of all the main stream channels. V_f ratio is calculated by $V_f = 2V_w / [(E_{ld} - E_{sc}) + (E_{rd} - E_{sc})]$ where V_w = valley floor width, E_{ld} and E_{rd} = left and

right side elevations of valley divides as you look down stream, and E_{sc} = stream channel or valley floor elevation. The classification of Vf-index was carried out using different values by El Hamdouni et al. (2007), Mahmood and Gloaguen (2012), and Fard et al. (2015). V_f index was categorized into three classes: class 1 ($V_f \leq 0.5$), class 2 ($0.5 \leq V_f < 1.0$), and class 3 ($V_f \geq 1.0$) (El Hamdouni et al. 2007). Mountain front sinuosity index (S_{mf}) is applied to check the effect of dominant force either tectonics or erosion on the topography. Mountain front sinuosity is computed by: $S_{mf} = L_{mf} / L_s$, where L_{mf} is

Fig. 2 Structural lineament map of the Kashmir Basin (Ali and Ali 2017)
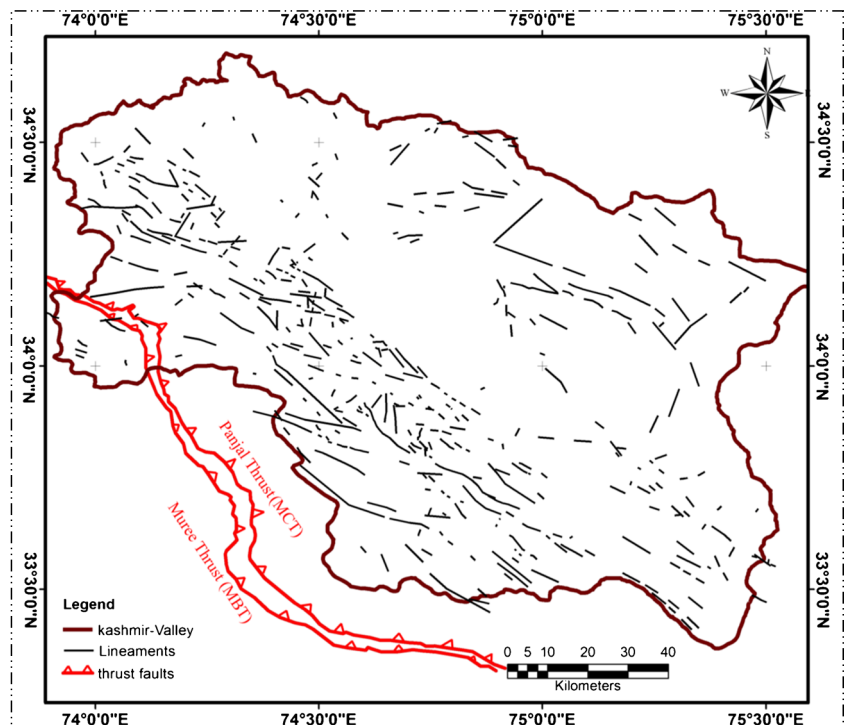
mountain front length at piedmont and L_s is straight length of front (Bull 1977; Bull 1978; Keller and Pinter 2002). *Smf* value were classified into class 1 with *Smf*<1.1, class 2 range from 1.1≤*Smf*<1.5, and class 3 with *Smf*≥1.5 (El Hamdouni et al. 2007). The asymmetric factor (A_f) is used to estimate tectonic tilting at the scale of a drainage basin (Keller and Pinter 2002; Hare and Gardner 1985). The asymmetry factor (A_f) is calculated as: $A_f = 100 (A_r/A_t)$, where A_f is the asymmetry index, A_t is total drainage basin area, and A_r is drainage basin area to the right side of master stream (looking downstream). The 14 Sub-watersheds of Sukhnag catchment were grouped into three classes: class 1: (A_f≥65 or A_f<35), class 2: (35≤A_f<43 or 57≤A_f<65), and class 3: (43≤A_f<57) (El Hamdouni et al. 2007). The horizontal projection of a basin is computed as basin shape index or the elongation ratio (B_s) (Ramírez-Herrera 1998; Cannon 1976) by $B_s = B_l / B_w$, where B_l is the basin length measured from the head to mouth, and B_w is the basin width measured at its widest point. Elongated basin shows high *Bs* values with relatively higher tectonic activity and circular basin shows low *Bs* value with low tectonic activity (El Hamdouni et al. 2007). The calculation of geomorphic indices for each sub-watershed was followed by computation of classes of relative active tectonics (Iat). Relative active tectonics (Iat) is carried out by taking average of different classes of geomorphic indices (S/n). Four classes of Iat depending on the level of tectonic influence in various sub-watersheds are class 1 is very high tectonic activity with S/n value range between 1 and 1.5; class 2 is high tectonic activity with S/n value of 1.5 S/n ≥ 1.5 but < 2; class 3 is moderately active tectonics with value of S/n ≥ 2 but < 2.5; and class 4 is low active tectonics with value of S/n ≥ 2.5 (El Hamdouni et al. 2007). The tectonic classes observed were supported by the correlation with tectonic lineaments (Ali and Ali 2017) and field evidences collected during the study.

Result and discussion

Geomorphic Indices

Stream length-gradient index (SL) and longitudinal river profiles

Stream length-gradient ratio can be used as sensitive indicator to examine the reach scale change in rock resistance, topography, and tectonic function. Streams flowing through different rocks and soils of strength variations tend to reach equilibrium with specific longitudinal profiles and hydraulic geometries (Bull 2007; Hack 1973). It can be applied to assess relative tectonic activity in a river basin (Dar et al. 2014; Zhang et al. 2011; Keller and Pinter 2002). The SL values for main channel were calculated from digital elevation model (DEM) in Arc GIS 10.2 software. The SL values range from

109 to 1875 (Fig. 3c) for Sukhnag river with anomalously high and low values over the geomorphic breaks originated by the tectonic activity, presence of hard and soft rocks; thus highlighting the structural influence on the topographic manifestation. Stream length-gradient index was calculated for sub-basin streams as well; the value ranges from 160 lowest for SF13 mouth side to 775 highest for SF7 present toward source side. The SL index was classified into three classes: class 1 (SL≥500), class 2 (300≤SL<500), and class 3 (SL<300) (El Hamdouni et al. 2007) shown in Fig. 3a. The high SL values are observed where rivers are crossing the hard rocks and other tectonic features and reveals comparatively high tectonic activity with convex profile. Alternatively, low SL values were associated with relatively low tectonic activity with softer and less-resistant underlying rocks (Keller and Pinter 2002; Hack 1973). The high SL values observed in terrain with underlying soft rocks also indicated influence of recent tectonic activity. Thus, the streams flowing from southwest side (higher altitudinal topography) showed higher stream length-gradient compared to streams flowing in northeast side (plainer topography) (Fig. 4a).

Moreover, the study of longitudinal river profiles of large streams are best representation of shape of valleys, which is usually smooth concave developed by action of rivers. Different geomorphic and tectonic processes of varying intensity have great influence on development of streams and their morphology. The analysis of longitudinal stream profiles provides evidences of lithological, tectonic, and fluvial processes dominating in the area. The longitudinal profile is an erosional curve used to interpret the surface history and different stage of valley growth from source to mouth. Analysis of stream profiles correlated with lineament distribution suggests more lineaments toward the Pir-Panjal side and unusual behavior of streams and stream beds in the form of knick points, and abrupt stream bending at lineament stream interaction. Moreover, dominance of more or less convex type stream profiles is attributed to higher tectonic activity than erosion in the area (Fig. 3b).

Hypsometric curve and integral (H_i)

The hypsometric integral (H_i) is elevation distribution across an area of land from one drainage basin to entire planet (Strahler 1952). The H_i is the area below the hypsometric curve, thus expresses the volume of a basin that has not been eroded. It is a useful tool to distinguish the areas showing tectonic activity and the area which are inactive (Keller and Pinter 1996).

The shape of hypsometric curve and the value of hypsometric integral not only supply useful information related to the erosional stage, but also on lithological, climatic, and tectonic variation controlling the basin (Huang and Niemann 2006; Molin et al. 2004). According to generated results, the
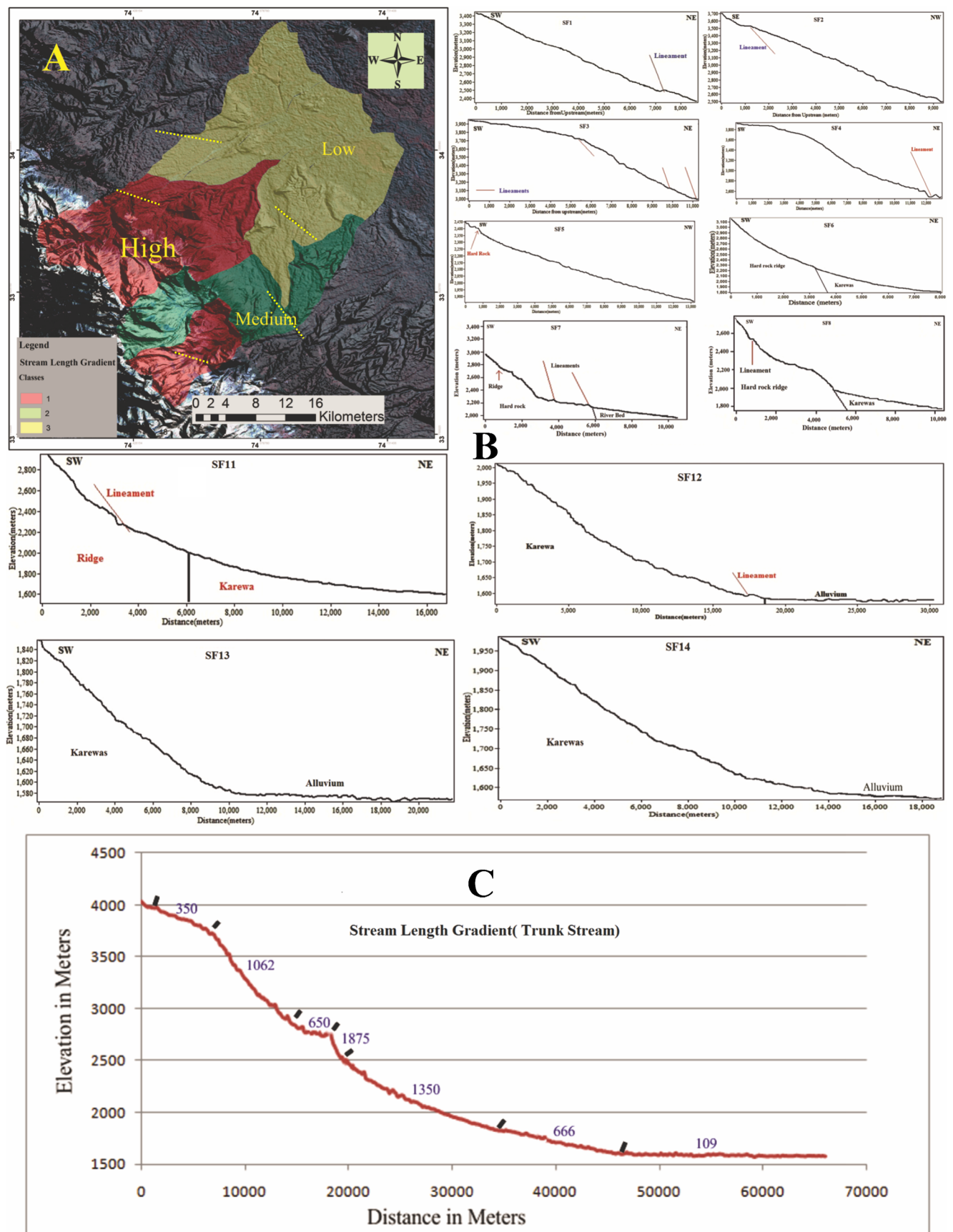
Fig. 3 Spatial variation in stream length-gradient ratio (**a**), longitudinal river profile of stream (**b**), and stream length-gradient ratio of Main River in the catchment (**c**)

H_i value showed range between 0.14 and 0.56. The H_i index was categorized into three classes based on convexity or concavity of the hypsometric curve: class 1 with convex curve ($H_i \geq 0.5$), class 2 with concave–convex curve ($0.4 \leq H_i < 0.5$), and class 3 with concave curve ($H_i < 0.4$). The Hi value calculated for the whole catchment is 0.509 and for sub-watersheds given in (Fig. 5a, b and Table 1), which indicates convex hypsometric curve. High values of the hypsometric integral are possibly related to young active tectonic, thus high values of index among 14 sub-watersheds highlighted that most of the area has high topography relative to the mean, possibly less eroded and younger terrain originated by active tectonic activity. Low values of H_i with concave curves are attributed to more eroded older landscape and less influenced by recent tectonics activity (Fig. 5b).

Valley floor width to height ratio (V_f)

Valley-floor width to height ratio is based on observation that areas with rapid uplift are cut by incised streams, narrow valley floors, and v-shaped valley profiles. High V_f value indicates wide and flat valley floor while as low V_f value pertains to actively uplifting v-shaped valleys. Evaluation of valley-floor width to valley height acts an indicator representing whether the stream is actively down cutting or mainly eroding laterally into the adjacent hill slopes. The V_f ratio range is 0.21 to 65.08 for different valley shapes. The areas with narrow and deep valleys have low V_f values < 1.0, are classified as "V"-shaped valleys and the areas showing V_f between 1 and 1.5 reveals moderately active, and the valleys with $V_f > 1.0$ can be classified as "U"-shaped valleys; these areas subject to major lateral erosion due to right lateral motion. The V_f index categorized into three classes are class 1 ($V_f \leq 0.5$), class 2 ($0.5 \leq V_f < 1.0$), and class 3 ($V_f \geq 1$) (El Hamdouni et al. 2007). These V_f values and valley shapes are shown in the map by V-shape and U-shape profiles. The V-shaped valleys indicate that the upstream tributaries are deeply incised while the U-shaped valleys indicate that the downstream side has flat valley floors (Fig. 6). The SW-side of the catchment showed V-shaped, deeply incised valleys which indicates the action of forceful tectonic activity.

Mountain front sinuosity (S_{mf})

The tectonic activity produces a straight front while as erosion cuts it into sinuous feature. S_{mf} reflects competing forces of tectonics and erosion. It can be applied to highlight the dominance of either tectonic or erosion forces. The S_{mf} values in an
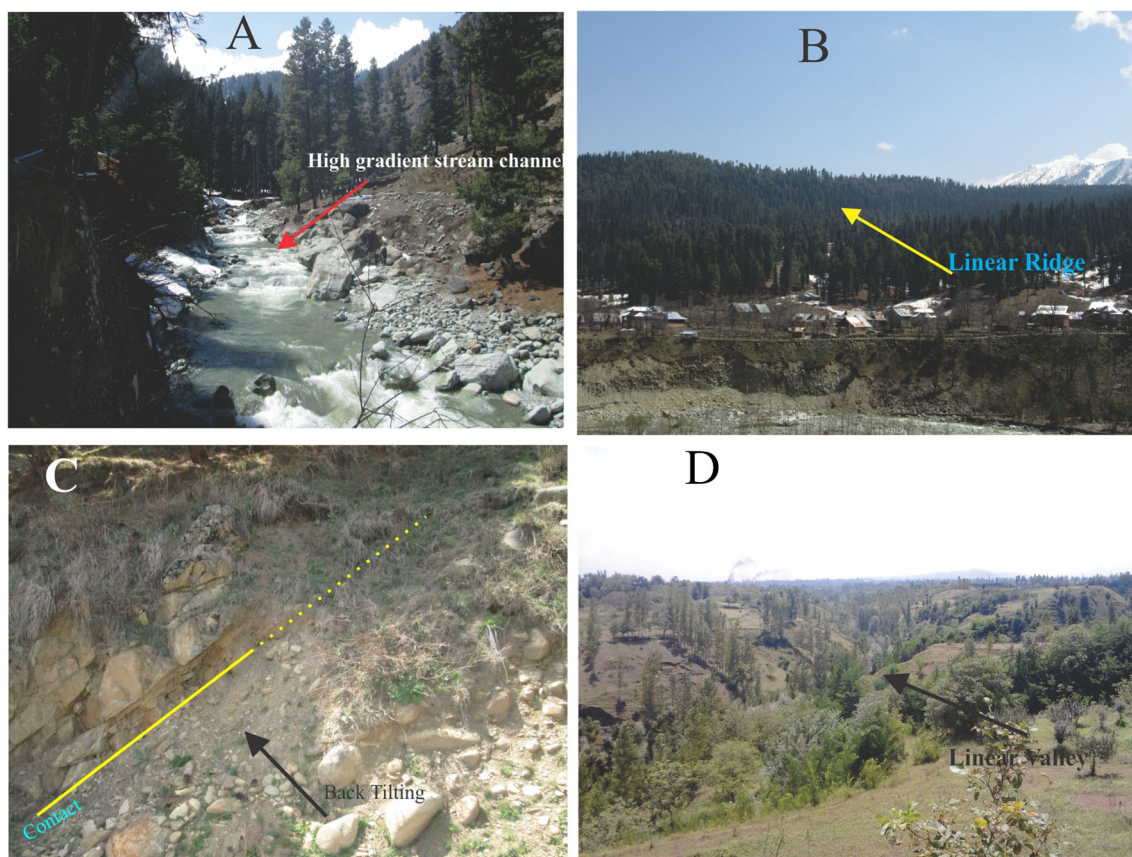
Fig. 4 Field evidence of some of the tectonic signatures observed at different places along the channel, **a** high gradient stream, **b** linear ridge, **c** back tilting, and **d** linear valley

Table 1 Hypsometric integral of 14 sub-watersheds

Sub-basin	Max. elevation(m)	Min. elevation (m)	Mean elevation (m)	Hypsometric integral (H_i)	Class
SF1	4176	2405	3391	0.5567476	1
SF2	4346	2434	3464	0.5387029	1
SF3	4460	3018	3745	0.5041609	1
SF4	4314	2456	3444	0.5317546	1
SF5	3177	1700	2363	0.4488829	2
SF6	3601	1801	2538	0.4094444	2
SF7	3827	1701	2586	0.4162747	2
SF8	3448	1776	2226	0.2691388	3
SF9	2508	1672	2019	0.4150718	2
SF10	1883	1574	1641	0.2168285	3
SF11	3619	1592	2032	0.2170696	3
SF12	2198	1571	1778	0.3301435	3
SF13	1857	1573	1613	0.1408451	3
SF14	2020	1572	1674	0.2276786	3

active regions range between 1.0 and 1.6, slightly active regions from 1.4 to 3.0, and inactive regions from 1.8 and > 5 (Bull and McFadden 1977). Some researchers have proposed that Smf index less than 1.4 are indication of tectonically active fronts (Rockwell et al. 1985; Burbank and Anderson 2001; Silva et al. 2003). Straight profiles with low S_{mf} value is indication of active fronts and irregular or more eroded profiles with high S_{mf} value is indication of less active fronts or inactive (Wells et al. 1988). Fourteen mountain fronts were selected and their S_{mf} was computed. The S_{mf} ranges from 1.095 to 2.244, and are given in Table 2 and Fig. 7. Most of the mountain fronts fall in tectonically active class, suggesting tectonically active nature with less dominance of erosion, although tectonics diminishes toward the plainer side (NE) of the catchment. This diminishing of tectonic activity toward plainer soft ground side can be due to obliteration of surface evidences of structures due to erosion with time.

Drainage basin asymmetry (A_f)

The asymmetric factor (A_f) can be applied to estimate tectonic tilting at the scale of a drainage basin (Keller and Pinter 2002; Hare and Gardner 1985). The A_f factor is close to 50 for basins developed under stable conditions with little or no tilting. This factor is sensitive to change in inclination perpendicular to the stream direction. A_f factor greater or less than 50 suggests tilt of the basin (Keller and Pinter 2002). The Af greater or less than 50 can be due the action of one or joint action of many of these as active tectonics, lithostructural control, differential erosion, e.g., the stream slipping down the bedding plains over time (El Hamdouni et al. 2008; Mahmood and Gloaguen 2012). The A_f value is 65.53 which infers that the master stream has left shift in the catchment. This drainage shift and basin tilting is also inferred as the right side tributaries are longer and the greater

number of tributaries joins the river. Drainage density of right side tributaries is high indicating uplift of basin to the right side (Fig. 8a). A_f factor varies from 22.97 (SF 5) to 77.25 (SF 9). The sub-watersheds were grouped into three classes: class 1: ($A_f \geq 65$ or $A_f < 35$), class 2: ($35 \leq A_f < 43$ or $57 \leq A_f < 65$), and class 3: ($43 \leq A_f < 57$) (El Hamdouni et al. 2007). The sub-watershed wise variation observed in A_f factor indicates that higher and lower A_f areas have been greatly influenced by the tilting caused along the active structures encountered in the area (Fig. 8b).

Basin shape index (B_s)

Tectonically active regions have relatively young drainage basins of elongated shape normal to topographic slope of a mountain. The areas of low tectonic processes or continued evolution, the basin shape changes from elongated to more circular (Bull and McFadden 1977). Bs was calculated from DEM and categorized into three classes: class 1 ($B_s \geq 4$), class 2 ($3 \leq B_s \leq 4$), and class 3 ($B_s \leq 3$) (El Hamdouni et al. 2007). The basins with high B_s are counted as elongated indicating relatively higher tectonic activity while basins with low B_s are counted as circular-shaped indicating relatively low tectonic activity. Elongated and steep basins are generally developed by rapidly uplifted mountain fronts; and widening of the basin occurs from the mountain front when tectonic activity diminishes or ceases (Bull and McFadden 1977; Ramírez-Herrera 1998). The calculation of B_s can reveal the rate of active tectonics of the area. The B_s index varies from 1.22 for (SF1) to 4.17 for (SF12) and has been categorized into 3 classes. The B_s index for Sukhnag catchment is 3.06. The sub-watersheds having B_s index greater than 3 indicates more or less elongated nature attributed to active tectonic impact.
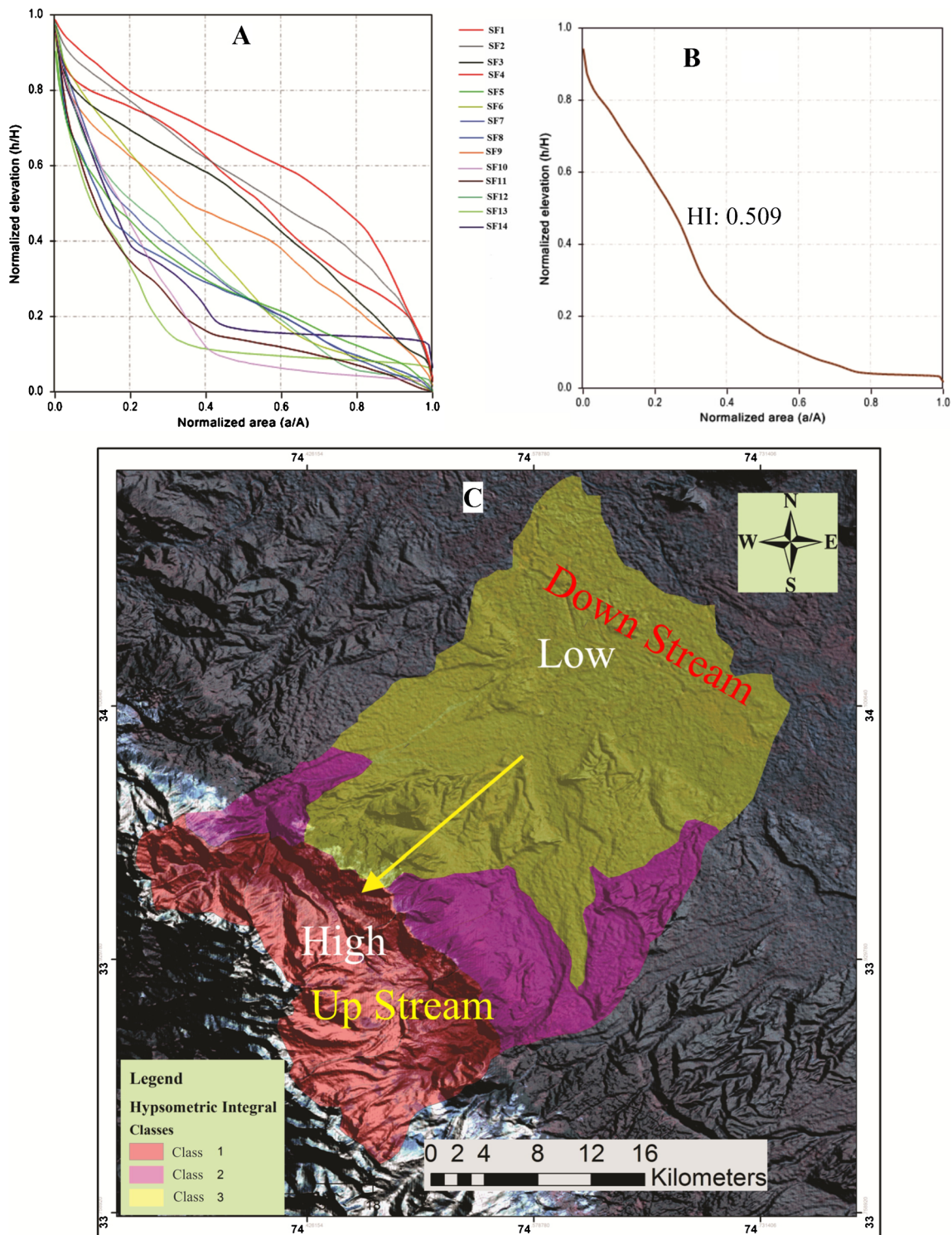
Fig. 5 Hypsometry curves. **a** Curve of 14 sub-watershed, **b** curve of whole catchment, and **c** Hi classes of whole catchment.

Relative tectonic activity (*Iat*)

The computations of geomorphic indices have helped to evaluate the tectonic activity in the study area. The role of the individual tectonic parameters and an average of these six indices were applied to assess the relative tectonic activity (*Iat*) and its distribution in the catchment (El Hamdouni et al. 2007). The relative tectonic activity (Iat) is obtained by the average of the different classes of geomorphic indices (S/n) computed under investigation of the present study. The earlier research on relative tectonic activity using geomorphic indices tends to focus on a particular mountain front or area (Azor et al. 2002; Bull
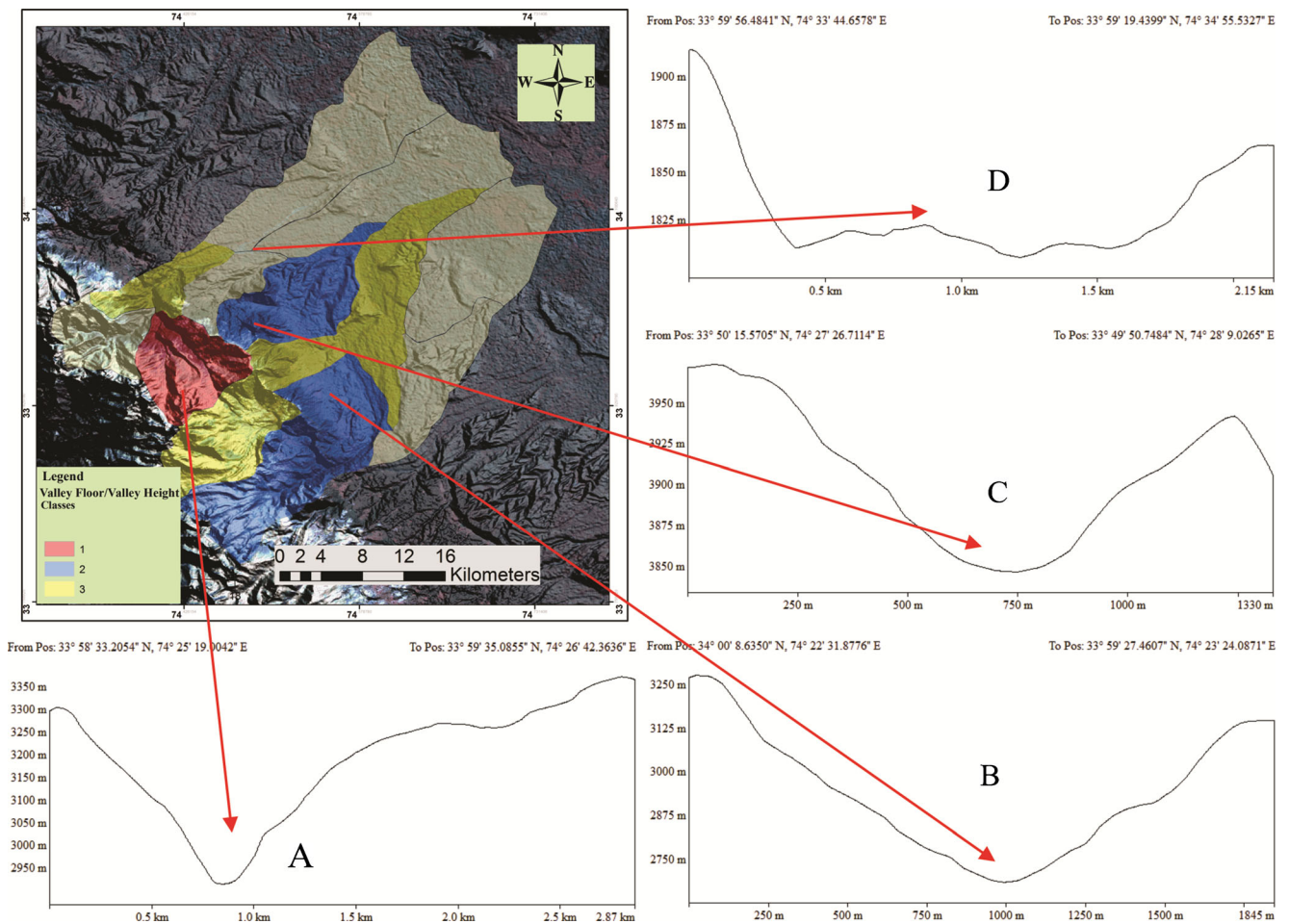
Fig. 6 Distribution map of valley floor width to height ratio with associated V-shaped valleys highly incised in upstream and U-shaped valleys in downstream side have flat valley floors

**Table 2** Mountain front Sinousity (S_{mf}) of Sukhnag catchment, Kashmir Basin

S No.	L_{mf}	L_s	$S_{mf} = L_{mf}/L_s$	Inference
1	19.8448	14.0305	1.416	Tectonically active
2	11.3223	9.52311	1.189	Tectonically active
3	11.0206	4.9121	2.244	Inactive settings
4	7.31669	4.91823	1.488	Slightly active
5	3.73421	3.41054	1.095	Tectonically active
6	5.24289	4.03313	1.299	Tectonically active
7	3.304	2.79847	1.181	Tectonically active
8	4.02781	3.29496	1.222	Tectonically active
9	1.20577	1.08057	1.116	Tectonically active
10	2.71528	2.34707	1.157	Tectonically active
11	5.6447	3.95396	1.428	Slightly active
12	11.6778	9.78312	1.194	Tectonically active
13	3.49443	2.91856	1.197	Tectonically active
14	3.17245	2.56697	1.236	Tectonically active

and McFadden 1977; Molin et al. 2004; Rockwell et al. 1985). The obtained values of geomorphic indices are categorized into four relative tectonic classes to depict the level of active tectonic influence; class 1 is very high tectonic activity with value ranging between (1.0≤Iat<1.5); class 2 is high tectonic activity based on values ranging between (1.5≤ Iat<2.0); class 3 shows moderate tectonic activity based on value ranging between (2.0≤ Iat<2.5); and class 4 with low tectonic activity with value of Iat≥2.5 (El Hamdouni et al. 2007). The 14 sub-watersheds have been divided into four tectonic activity classes based on the Iat values. In the four relative active tectonic classes, no sub-watershed falls in class 1, i.e., very high active tectonic class. About 33.96% (331.505 km^2) in class 2; 32.40% (316.255 km^2) in class 3; and 33.54% (327.351 km^2) in class 4 category of relative active tectonics.

Lineament analysis and field evidence

Lineaments of tectonic significance were delineated using false color composite (FCC), edge enhancement filters, and DEM-derived product to infer the tectonic behavior of
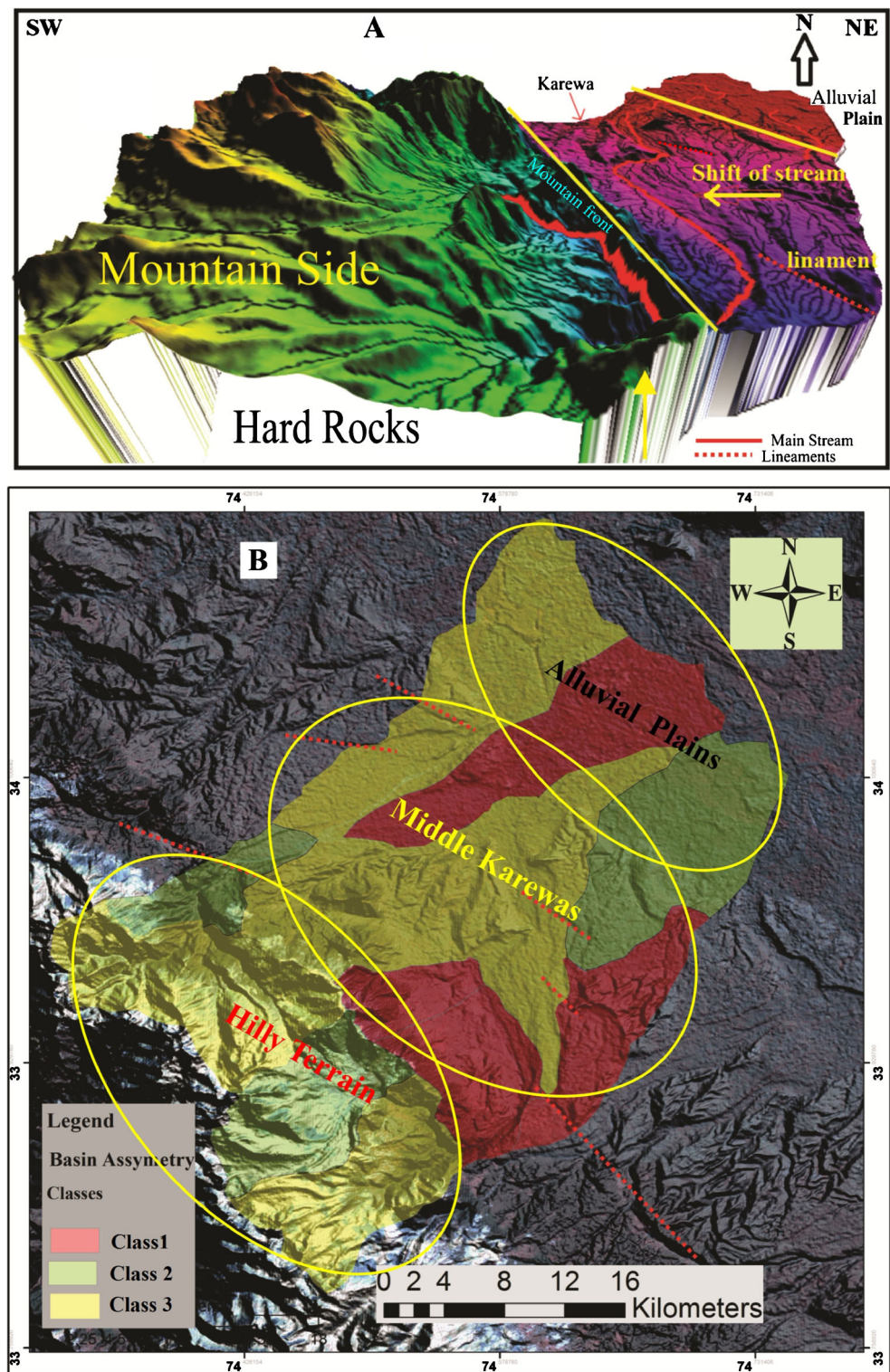
Fig. 7 Mountain fronts sinuosity
(Smf)
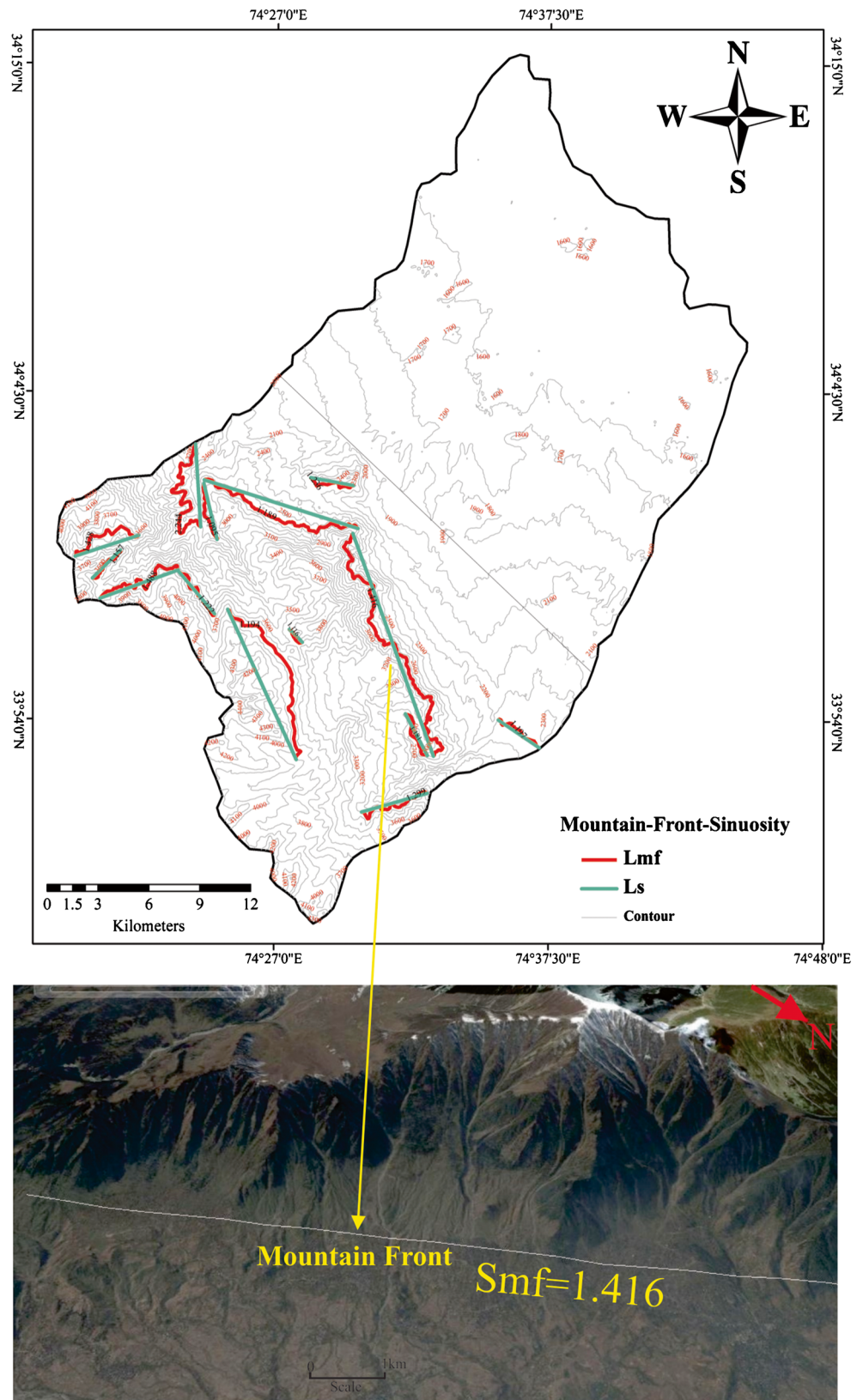
seismically active Kashmir basin (Ali and Ali 2017). Lineament map shows high lineament density toward Pir-

Panjal side and low density in alluvial floor of the watershed. Pir-Panjal side in its southwest shows a complex pattern of

Fig. 8 **a** Drainage shift, basin tilting. **b** Drainage basin asymmetry variation of 14 sub-watersheds

faulting with the superposition of several thrusts from northeast to southwest are, the MCT/Panjal thrust, MBT/Murree thrust, Riasi thrust, and Kotli thrust (Thakur et al. 2010). The lineament density showed maximum correlation with the regional tectonic structures and high density earthquake zones surrounding the Kashmir Basin (Shah 2013; Ali and Ali

2017) (Fig. 9). Moreover, the faults like Balapur fault (Ahmad et al. 2013; Ahmad and Bhat 2012), Tosamaidan Fault, and other linear structures showed dominantly NW to SE trend investigated using rose diagrams (Ali and Ali 2017), linearly related with of distribution of earthquake epicenters in the surroundings.

Lineament mapping is valuable element to recognize the tectonic behavior of the area (Kassou et al. 2012). The sub-watersheds with presence of structural features/lineaments showed higher relative tectonic activity. The parts of catchment which shows high density of tectonic lineaments concords with the tectonic behavior recognized by computation of relative tectonic activity. The area with higher lineament density falls in class 2, i.e., high tectonic activity based on values of geomorphic indices in Iat computation. A lot of field evidences were found associated with the lineaments in high tectonic activity area dominated by V shaped valleys (Fig. 4d), back tilting (Figs. 4c, 10d), linear mountain fronts, linear valleys and ridges (Fig. 4b, d), and steeply dipping rock formations (Fig. 10c) can be geomorphic evidence of recent tectonic activity. The high tectonic activity area showed number of rock deformations and vertical displacement evidences in the form of fault offsets (Fig. 10b) and macro-folds (Fig. 10a) highlighting the effect of recent uplift of Pir-Panjal on the Kashmir basin. Moreover, the area showed dominantly soft-sediment deformation structures (Ali and Ali 2018), intense folding (Fig. 10e), micro-faulting, and sills with shuttered bounding surfaces are possible evidences developed by the effect of paleo-earthquake vibrations in the Kashmir Basin. Tectono-geomorphic features and earthquake distribution pattern are associated and strongly controlled by the regional tectonic structures responsible for the seismic hazard (Ali and Ali 2020). Moreover, the effect of faults on terrain was observed with active moments uplifting the southwest side and subsiding the northeast side of Kashmir basin (Shah 2013).

Conclusion

The investigated catchment is part of Kashmir basin lying in seismically active zone, NW Himalaya. The computation of geomorphic indices have proven useful tool in evaluating relative tectonic activity. The geomorphic indices computed for assessing the relative tectonic index (Iat) was performed by the combination of geomorphic indices. The total area is divided in four classes using the Iat-Index. In the four relative active tectonic classes, no sub-watershed falls in class 1, i.e., very high active tectonic class. About 33.96% (331.505 km^2) of area falls in class 2; 32.40% (316.255 km^2) to class 3; and 33.54% (327.351 km^2) to class 4. More than half of the area falls in class 2 and 3, i.e., high to moderate tectonic activity. The sub-watersheds of high to moderate tectonic activity were found in which a number of structural lineaments and other structural features showed their presence and influence on geomorphic manifestation. The SL and Hi values at some places were very high, which indicates an indication of folding and faulting. Moreover, straight and deep narrow valleys,
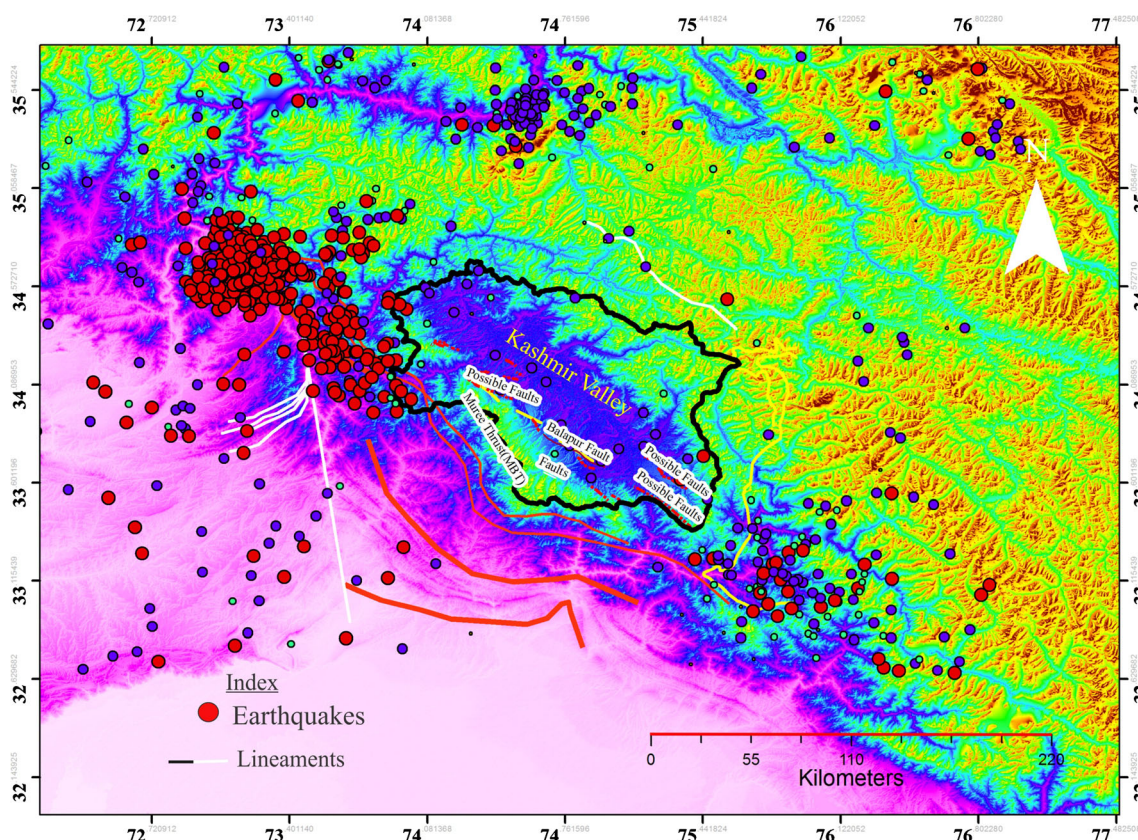
Fig. 9 Regional tectonic structures and high density earthquake zones surrounding the Kashmir Basin

Fig. 10 Field evidences encountered in the area: **a** macro-folding, **b** sand sills with upper and lower shuttered surfaces associated with faulting, **c** steeply dipping lithology, **d** back tilting in Karewas, and **e** intense folding in Lower Karewas toward Pir-Panjal side
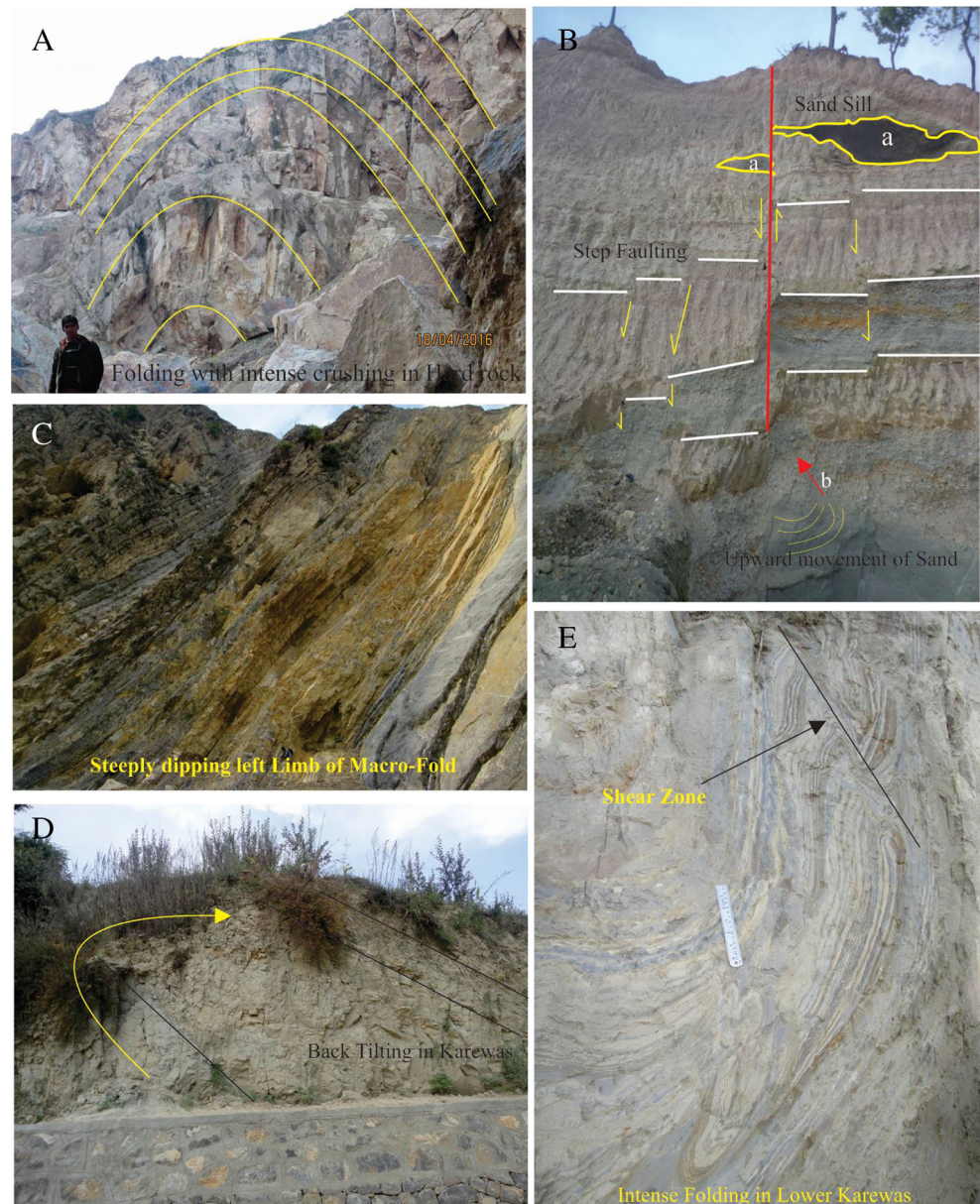
and deformed deposits were found in these high to moderate tectonic areas. The Vf-index suggests high incision rate linked with tectonic uplift which developed the deep and narrow valleys. Various field evidences support the active tectonics in parts of the catchment and showed concordance with the value of active tectonic indices and classes based on Iat index. During the field investigation along the structural lineaments in high tectonic areas, deformation was observed in the form of fault-offsets, back tilting and folding, and other geomorphic anomalies like stream deflection, straight streams, and knick points in various longitudinal river profiles at lineament crossing. Thus, the present study helped in evaluating the relative tectonic activity of seismically active area, NW Himalaya.

Declarations

References

Ahmad S, Bhat MI (2012) Tectonic geomorphology of the Rambiara basin, SW Kashmir Valley reveals emergent out-of-sequence active fault system. Himal Geol 33:162–172

Ahmad S, Bhat MI, Madden C, Bali BS (2013) Geomorphic analysis reveals active tectonic deformation on the eastern flank of the Pir Panjal Range, Kashmir Valley, India. Arab J Geosci 7:2225–2235. https://doi.org/10.1007/s12517-013-0900-y

Ali SA, Ali U (2017) Evaluating linear geological structures in seismogenic compressional setting Kashmir basin, NW-Himalaya. Spat Inf Res 6:801–811

Ali U, Ali SA (2018) Seismically induced soft-sediment deformation structures in an active seismogenic setting: The Plio-Pleistocene Karewa deposits, Kashmir Basin (NW Himalaya). J Struct Geol 115:28–46

Ali U, Ali SA (2020) Comparative response of Kashmir Basin and its surroundings to the earthquake shaking based on various site effects. Soil Dyn Earthq Eng 132:1–17

Ambraseys NN (2004) A note on three little-known early earthquakes in India. Curr Sci 86(4):506–508

Azor A, Keller EA, Yeats RS (2002) Geomorphic indicators of active fold growth: South Mountain-Oak Ridge Ventura basin, southern California. Geol Soc Am Bull 114:745–753

Bali BS, Wani AA (2021) Analysis of neotectonic structures in the piedmont region of Pir Panjal Range NW Himalaya by integrating geomorphic indicators coupled with geophysical transects (GPR). Nat Hazards 105(3):2869–2882

Bali BS, Wani AA, Khan RA, Ahmad S (2016) Morphotectonic analysis of the Madhumati watershed, northeast Kashmir Valley. Arab J Geosci 9(5). https://doi.org/10.1007/s12517-016-2395-9

Bathrellos GD, Antoniou VE, Skilodimou HD (2009) Morphotectonic characteristics of Lefkas Island during the quaternary (Ionian Sea, Greece). Geol Balcanica 38:23–33

Bilham R (2004) Earthquakes in India and the Himalaya: Tectonics, geodesy and history. Ann Geophys 47:839–858

BIS Code 1893 (2002) Earthquake hazard zoning map of India. www.bis.org.in

Brown LD, Zhao W, Nelson KD, Hauck M, Alsdorf D, Ross A, Cogan M, Clark M, Liu X, Che J (1996) Bright Spots, Structure, and Magmatism in Southern Tibet from INDEPTH Seismic Reflection Profiling. Science 274(5293):1688–1690

Bull WB (1977) The alluvial-fan environment. Prog Phy Geography 1–2:222–270

Bull WB (1978) Geomorphic tectonic classes of the south front of the San Gabriel Mountains, California. U.S. Geological Survey Contract Report, 14-08-001-G-394, Office of Earthquakes, Volcanoes and Engineering, Menlo Park, CA.

Bull WB (2007) Tectonic geomorphology of mountains: a new approach to Paleoseismology. Blackwell

Bull W, McFadden L (1977) Tectonic geomorphology north and south of the Garlock Fault, California. In: Doehring DO (Ed.), Geomorphology in Arid Regions, Geomorphology, p 115–138. https://doi.org/10.4324/9780429299230-5

Burbank DW, Anderson RS (2001) Tectonic geomorphology, 1st edn. Blackwell Science Ltd., Australia, p 160

Cannon PJ (1976) Generation of explicit parameters for a quantitative geomorphic study of Mill Creek drainage basin. Oklahoma Geology Notes 36(1):3–16

Chen YC, Sung Q, Cheng KY (2003) Along-strike variations of morphotectonic features in the Western Foothills of Taiwan: tectonic implications based on stream-gradient and hypsometric analysis. Geomorphology 56:109–137

Cox RT (1994) Analysis of drainage-basin symmetry as a rapid technique to identify areas of possible Quaternary tilt-block tectonics: An example from the Mississippi Embayment. Geol Soc Am Bull 106(5):571

Crevenna AB, Rodrı́gueza VT, Soranic V, Framed D, Ortiz MA (2005) Geomorphometric analysis for characterizing landforms in Morelos State, Mexico. Geomorphology 67:407–422

Dar RA, Romshoo SA, Chandra R, Ahmad I (2014) Tectono-geomorphic study of the Karewa Basin of Kashmir Valley. J Asia Earth Sci 92:143–156

DeCelles PG, Robinson DM, Quade J, Ojha TP, Garzione CN, Copeland P, Upreti BN (2001) Stratigraphy, structure, and tectonic evolution of the Himalayan fold-thrust belt in western Nepal. Tectonics 20(4):487–509

El Hamdouni R, Irigaray C, Fernandez T, Chacón J, Keller EA (2007) Assessment of relative active tectonics, southwest border of Sierra Nevada (southern Spain). Geomor 96:150–173

El Hamdouni R, Irigaray C, Fernández T, Chacón J, Keller EA (2008) Assessment of relative active tectonics, southwest border of Sierra Nevada (Southern Spain). Geomor 96:150–173. https://doi.org/10.1016/j.geomorph.2007.08.004

Fard NG, Sorbi A, Arian M (2015) Active tectonics of Kangavar area, West Iran. Open J Geol 5:422–441. https://doi.org/10.4236/ojg.2015.56040

Gansser A (1964) Geology of the Himalaya. Interscience Publishers, Landon, p 289

Gloaguen R, Marpu PR, Niemeyer I (2007) Automatic extraction of faults and fractal analysis from remote sensing data. Nonlinear Process Geophys 14(2):131–138

Gloaguen R, Kaessner A, Wobbe F, Shahzad F, Mahmood SA (2008) Remote sensing analysis of crustal deformation using river networks. In: IEEE International Geosciences and Remote Sensing Symposium, Boston. pp. IV-1–IV-4

Hack JT (1973) Stream-profiles analysis and stream-gradient index. J Research of the US Geological Sur 1(4):421–429

Hare PH, Gardner TW (1985) Geomorphic indicators of vertical neotectonism along converging plate margins, Nicoya Peninsula, Costa Rica. In: Morisawa M, Hack JT (eds) Tectonic Geomorphology. Allen and Unwin, Boston pp, p 75e104

Howard AD (1967) Drainage Analysis in Geologic Interpretation: A Summation. AAPG Bulletin 51

Huang XJ, Niemann JD (2006) Modelling the potential impacts of groundwater hydrology on long-term drainage basin evolution. Earth Surf Pro Landforms 31:1802–1823

Jain AK, Sandeep S, Manickavasagam RM (2002) Himalayan Collision Tectonics. Gondwana research group Memoir, 7, p 114

Jain AK, Manickavasagam RM, Singh S, Mukherjee S (2005) Himalayan Collision zone: new perspectives – its tectonic evolution in a combined ductile shear zone and channel flow model. Himalayan Geol 26(1):1–8

Kamberis E, Bathrellos GD, Kokinou E, Skilodimou HD (2012) Correlation between the structural pattern and the development of the hydrographic network in a portion of the Western Thessaly Basin (Greece). Cent Euro J Geosci 4(3):416–424

Kaneda H, Nakata T, Tsutsumi H, Kondo H, Sugito N, Awata Y, Akhtar SS, Majid A, Khattak W, Awan AA, Yeats RS, Hussain A, Ashraf M, Wesnousky SG, Kausar AB (2008) Surface rupture of the 2005 Kashmir, Pakistan, earthquake and its active tectonic implications. Bull Seismol Soc Am 98(2):521–557

Kassou A, Essahlaoui A, Aissa M (2012) Extraction of structural lineaments from satellite images Landsat7 ETM+ of Tighza mining district (Central Morocco). Research J of Earth Sci 4(2):44–48

Keller EA, Pinter N (1996) Active tectonics: earthquakes, uplift and landscape, first edn. Prentice Hall, New Jersey, p 156

Keller EA, Pinter N (2002) Active tectonics: earthquakes, uplift, and landscape, second edn. Prentice Hall, New Jersey, p 1e362

Kurz T, Gloaguen R, Ebinger C, Casey M, Abebe B (2007) Deformation distribution and type in the Main Ethiopian Rift (MER): A remote sensing study. J African Earth Sci 48 (2–3):100–114

Ma J, Dong L, Zhao G, Li X (2018) Qualitative method and case study for ground vibration of tunnels induced by fault-slip in underground mine. Rock Mech Rock Eng 52:1887–1901

Ma J, Dong L, Zhao G, Li X (2019) Ground motions induced by mining seismic events with different focal mechanisms. Int J Rock Mech Min Sci 116:99–110

Madden C, Trench D, Meigs A (2010) Late quaternary shortening and earthquake chronology of an active fault in the Kashmir Basin, Northwest Himalaya. Seismol Res Lett 81(2):346

Madden C, Ahmad S, Meigs A (2011) Geomorphic and paleoseismic evidence for late quaternary deformation in the southwest Kashmir Valley, India: out-of-sequence thrusting, or deformation above a structural ramp? American Geophysical Union abstracts T54B-07

Malik JN, Mohanty C (2007) Active tectonic influence on the evolution of drainage and landscape: Geomorphic signatures from frontal and hinterland areas along the Northwestern Himalaya, India. J Asian Earth Sci 29(5–6):604–618

Mahmood SA, Gloaguen R (2012) Appraisal of active tectonics in Hindu Kush: insights from DEM derived geomorphic indices and drainage Analysis. Geosci Front 3(4):407–428. https://doi.org/10.1016/j.gsf.2011.12.002

Meigs A, Madden C, Yule JD, Gavillot Y, Hebeler A, Hussain A, Bhat MI, Kausar AB, Malik M, Ramzan S, Sayab M, Yeats R (2010) Distributed deformation, distributed earthquakes in the northwest Himalaya. 25th Himalaya–Karakoram–Tibet Workshop, San Francisco, U.S. Geological Survey Open File Rep. 2010–1099, 129–130

Molin P, Pazzaglia FJ, Dramis F (2004) Geomorphic expression of active tectonics in a rapidly-deforming forearc, sila massif, Calabria, southern Italy. American J Sci 304:559–589

Molnar P, Tapponnier P (1975) Cenozoic Tectonics of Asia: Effects of a Continental Collision: Features of recent continental tectonics in Asia can be interpreted as results of the India-Eurasia collision. Science 189(4201):419–426

Nakata T (1972) Geomorphic history and crustal movement of the foot-hill of the Himalaya. Science Report, Tohoku University, 7th ser. (Geogr) 22:39–177

Nakata T (1986) Active faults in the Himalayan ranges and their tectonic significance. In: Saklani PS (Ed) Himalayan thrust and associated rocks, current trends in Geology, today and tomorrow's Publications, Delhi, 9:203–208

Nakata T (1989) Active faults of the Himalaya of India and Nepal. Geol Soc Am Spec Pap 232:243–264

Nakata T, Iwata S, Yamanaka H, Yagi H, Maemoku H (1984) Tectonic landforms of several active faults in the western Nepal Himalaya. J Nepal Geological Society 4:177–200

Ohmori H (1993) Changes in the hypsometric curve through mountain building resulting from concurrent tectonics and denudation. Geomor 8:263–277

Philip G, Virdi NS (2006) Co-existing compressional and extensional regimes along the Himalayan front vis-à-vis active faults. Curr Sci 90(9):1267–1271

Pike RJ, Wilson SE (1971) Elevation–relief ratio, hypsometric integral and geomorphic area-altitude analysis. Geol Soc Am Bull 82:1079–1084

Ramírez-Herrera MT (1998) Geomorphic assessment of active tectonics in the Acambay Graben, Mexican volcanic belt. Earth Surface Proc Landforms 23:317–332

Riquelme R, Martinod J, Hérail G, Darrozes J, Charrier R (2003) A geomorphological approach to determining the Neogene to Recent tectonic deformation in the Coastal Cordillera of northern Chile (Atacama). Tectonophysics 361(3–4):255–275

Rockwell TK, Keller EA, Johnson DL (1985) Tectonic geomorphology of alluvial fans and mountain fronts near Ventura, California. In: Morisawa M (ed) Tectonic Geomorphology. Proceedings of the 15th Annual Geomorphology Symposium. Allen and Unwin Publishers, Boston, pp 183–207

Schelling D, Arita K (1991) Thrust tectonics, crustal shortening, and the structure of the far-eastern Nepal Himalaya. Tectonics 10(5):851–862

Shah AA (2013) Earthquake geology of Kashmir Basin and its implications for future large earthquakes. Int J Earth Sci 102:1957–1966

Shah, AA (2015a) Comment on: "Macroseismic intensity assessment of 1885 Baramulla Earthquake of northwestern Kashmir Himalaya, using the Environmental Seismic Intensity scale (ESI 2007)". Quat. Int. 355, 172–174

Shah AA (2015b) Comment on: Alam Akhtar, Ahmad Shabir, Sultan Bhat, M., Ahmad Bashir, 2015. Tectonic evolution of Kashmir basin in northwest Himalayas. Geomorphology, 239, 114-126. https://doi.org/10.1016/j.geomorph.2015.03.025

Silva PG, Goy JL, Zazo C and Bardaj'ı T (2003) Fault generated mountain fronts in south-east Spain: geomorphologic assessment of tectonic and seismic activity; Geomor 50: 203–225.

Srikantia SV, Bhargava ON (1998) Geology of Himachal Pradesh. J Geological Society of India, p 416

Strahler AN (1952) Hypsometric (area–altitude) analysis of erosional topography. Geol Soc Am Bull 63:1117–1142

Thakur VC (1993) Geology of the western Himalaya. Pergmon press, Oxford and New York, p 355

Thakur VC (2004) Active tectonics of Himalayan Frontal Thrust and Seismic Hazard to Ganga Plain. Current Sci 86(11):1554–1560

Thakur VC, Jayangondaperumal R, Malik MA (2010) Redefining Medlicott–Wadia's main boundary fault from Jhelum to Yamuna: an active fault strand of the main boundary thrust in northwest Himalaya. Tectonophysics 489:29–42. https://doi.org/10.1016/j.tecto.2010.03.014

Toudeshki VH, Arian M (2011) Morphotectonic Analysis in the Ghezel Ozan River Basin, NW Iran. J Geogr Geol 3(1)

Valdiya KS (1980) Geology of Kumaun Lesser Himalaya. Wadia Institute of Himalayan Geology, Dehradun, U.P., p 291

Valdiya KS (1992) The main boundary thrust zone of Himalaya, India. Ann Tectonics 6:54–84

Valdiya KS (1998) Late Quaternary movements and landscape rejuvenation in southeastern Karnataka and adjoining Tamil Nadu in Southern Indian shield. J Geol Soc India 5l(2):139–166

Valdiya KS (2001) Reactivation of Terrane-Defining boundary Thrusts in central sector of the Himalaya implications. J Curr Sci 81: 1418–1431

Wani AA, Bali BS (2017) Geomorphic analysis of relative tectonic activity in the Sindh Basin, Jammu and Kashmir Himalaya, northwest India. J Himal Geol 38(2):171–183

Wani AA, Bali BS, Mohammad S (2019) Drainage characteristics of tectonically active area: an example from Mawar Basin, Jammu and Kashmir, India. J Geol Soc India 93(3):313–320

Wani AA, Bali BS, Bhat GR, Hussain N (2020) Impact of tectonics on drainage network evolution of Suru basin, Kargil N/w Himalaya, Jammu and Kashmir, India. Environ Earth Sci 79(1)

Wells SG, Bullard TF, Menges TM, Drake PG, Karas PA, Kelson KI, Ritter JB, Wesling JR (1988) Regional variations in tectonic geomorphology along segmented convergent plate boundary, Pacific coast of Costa Rica. Geomor 1:239–265

Yousuf M, Bukhari SK (2020a) Evaluation of seismically induced Soft Sediment deformation structures vis-a-vis their probable earthquake sources in Kashmir basin, NW Himalaya. J Earthquake and Tsunami 15(1):2150003. https://doi.org/10.1142/S1793431121500032

Yousuf M, Bukhari SK (2020b) Hazard Estimation of Kashmir Basin, NW Himalaya using probabilistic seismic hazard assessment. Acta Geophysica 68(5):1295–1316

Yousuf M, Bukhari SK, Bhat GR, Ali A (2020) Understanding and managing earthquake hazard visa viz disaster mitigation strategies in Kashmir valley, NW Himalaya. Progress in Disaster Science 5: 100064

Zhang W, Hayakawa YS, Oguchi T (2011) DEM and GIS based morphometric and topographic-profile analyses of Danxia landforms. Geomorphom Org:121–124